THE ASTROPHYSICAL JOURNAL, 268:134–144, 1983 May 1

HIGH-VELOCITY, ASYMMETRIC DOPPLER SHIFTS OF THE X-RAY EMISSION LINES OF CASSIOPEIA A

T. H. MARKERT, C. R. CANIZARES,[1] AND G. W. CLARK
Department of Physics and Center for Space Research, Massachusetts Institute of Technology
AND
P. F. WINKLER
Department of Physics, Middlebury College
Received 1982 August 9; accepted 1982 October 22

ABSTRACT

Using the Focal Plane Crystal Spectrometer on the *Einstein Observatory*, we have performed high spectral resolution measurements of several X-ray emission lines from the young supernova remnant Cassiopeia A. The spectrum of the X-ray emitting gas in the northwest half of Cas A is redshifted with respect to that in the southeast. We interpret this phenomenon as a Doppler shift and find the mean velocity difference between the two regions to be 1820 ± 290 km s^{-1}. Within each region the breadth of the X-ray lines implies a Doppler broadening of ~ 5000 km s^{-1} (FWHM). These measurements demonstrate directly that the bulk of the gas making up Cas A is moving at high velocities.

We have constructed a simple geometric model consistent with the general features of the X-ray spectrum and image of Cas A—a broad ring of matter inclined to the line of sight. The data constrain the parameters of the model and in particular require an expansion velocity in excess of 2000 km s^{-1}.

The high velocities required for the X-ray matter (and the consequently high temperature of the primary shock) imply that the relatively cool X-ray emitting material that we observe is most probably supernova ejecta which has been heated by a reverse shock wave. Although alternative scenarios cannot be excluded, the X-ray and optical data are most compatible with the view that Cas A is still in its free-expansion stage. We find that the X-ray emitting mass is probably $\gtrsim 10\ M_\odot$ as previously determined by others, and the kinetic energy is $\sim 4 \times 10^{51}$ ergs.

The spatial and Doppler asymmetries may be caused by modest inhomogeneities either in the distribution of circumsource material or in the ejecta themselves, as has been suggested for rapidly rotating massive stars.

Subject headings: nebulae: individual — nebulae: supernova remnants — X-rays: sources — X-rays: spectra

I. INTRODUCTION

The dynamics of the supernova remnant Cas A have been studied by observations of the Doppler shifts in the optical emission lines (van den Bergh 1971) and from studies of proper motions of optical filaments and of features in radio maps (Kamper and van den Bergh 1976; Bell 1977). The optical measurements are the more accurate, but are limited to a few bright features (the so-called fast-moving knots, with $v \sim 6000$ km s^{-1}, and the quasi-stationary flocculi with $v \lesssim 1500$ km s^{-1}; Baade and Minkowski 1954) which have a total mass $\lesssim 0.1\ M_\odot$, a small fraction of the total mass of the supernova ejecta. The radio studies reveal lower apparent velocities ($\lesssim 1500$ km s^{-1}) perpendicular to the line of sight (Bell 1977; Tuffs 1982), although the radio picture is so chaotic that the proper motion is at best a global average with many large deviations from the mean motion (Angerhofer 1982).

In recent years Cas A has been observed extensively at X-ray wavelengths. Observations made with the High Resolution Imager (HRI) and the Imaging Proportional Counter (IPC) on the *Einstein Observatory* (Giacconi *et al.* 1979; Murray *et al.* 1979; Fabian *et al.* 1980) have provided maps which suggest that the X-ray emission originates in two concentric thin shells. By assuming a simple model, one finds the mass of the X-ray emitting matter to be of order 10–20 $M_\odot$, considerably more than observed optically. Thus, X-ray measurements probe the bulk of the material in the supernova remnant.

Moderate resolution X-ray spectra ($\Delta E \sim 160$ eV) of Cas A were obtained with the solid state spectrometer (SSS) on *Einstein* (Becker *et al.* 1979). Emission lines from highly ionized sulfur, silicon, argon and several other elements were clearly detected. These spectra are consistent with models in which the remnant contains gas

[1] Alfred P. Sloan Research Fellow; also Institute of Astronomy, University of Cambridge.

at two different temperatures ($kT = 0.62$ and 4.0 keV). The emission measure of the low-temperature component is 7.5 times that of the high-temperature component.

Spectral measurements made with the Bragg spectrometer (Focal Plane Crystal Spectrometer = FPCS) on *Einstein* are described here. The high energy resolution ($E/\Delta E \gtrsim 100$) of the FPCS permits the measurement of closely spaced emission lines and the determination of small shifts in energy from nominal values. We report here measurements of energy shifts of several X-ray emission lines observed in Cas A. As in the case of the optical measurements, we interpret these as Doppler shifts due to velocities of the X-ray emitting matter along the line of sight. Unlike the optical photons, however, the X-rays arise from the bulk of the Cas A material. With this information and the HRI image we are able to make reasonable deductions about the dynamics of Cas A and its three-dimensional structure.

II. OBSERVATIONS

In this paper we will consider observations of only those lines (or sets of lines) which were found to be reasonably bright in the SSS data (Becker *et al.* 1979) and which are separated in energy from other lines sufficiently so that they can be identified and measured without confusion. These are the helium-like triplets of silicon and sulfur (Si XIII and S XV) and the Lyman-α line of hydrogen-like sulfur (S XVI). The specific transitions and some of the details of the observations are shown in Table 1. FPCS observations of other lines will be reported separately.

The FPCS instrument has been described in detail elsewhere (Canizares *et al.* 1977, 1979). Briefly, it is a curved-crystal Bragg spectrometer. X-rays focused by the *Einstein* telescope strike one of six diffractors. X-rays with wavelengths very near those specified by the Bragg condition are refocused astigmatically onto a position-sensitive proportional counter. The optics of the system are such that information on the position of the X-ray source in one dimension is available with an angular resolution of 1′–2′.

Most of the X-ray emission from Cas A was shown by Murray *et al.* (1979) to come from an incomplete inner shell of diameter ~4′. A contour plot of the HRI image (Fig. 1) shows that the shell can be crudely characterized as two bright lobes in the northwest and southeast. The orientation of the spacecraft during the FPCS observation was such that these two lobes were spatially resolved from one another; the line in Figure 1 shows the division we have made for this analysis.

In order to achieve the maximum spectral resolution afforded by the FPCS when observing a spatially extended X-ray source such as Cas A, it is necessary to correct the observed spectrum for effects which arise from the finite angular extent of the source (Winkler *et al.* 1981). These corrections may be checked by independently observing the source through a narrow aperture, thereby limiting the spatial extent in one dimension (the effects due to the angular size of the object are important only in the imaging direction). For one set of observations of the Si XIII lines in Cas A, a 2′ × 20′ aperture was placed at the focus and the telescope was pointed so that each half of the nebula was imaged separately. The results obtained from these narrow-aperture observations are entirely consistent with those in which the entire remnant was studied. Therefore, we have confidence that the procedure used to correct the observed spectrum is valid.

III. RESULTS

The immediate conclusion we draw from the FPCS observations of Cas A is that there is a significant shift in the X-ray spectrum of the NW half of Cas A in comparison to that of the SE. The only plausible explanation for this phenomenon is as a Doppler shift arising from different bulk radial velocities of the X-ray emitting gas in the two regions. We find the mean radial velocity difference to be ~ 1800 km s^{-1}.

The spectral shifts are illustrated in Figures 2–4, where we have plotted the counting rate histograms for each of the four observations listed in Table 1. In each case the spectrum of NW lobe of Cas A peaks at a slightly lower energy than that of the SE lobe.

In order to verify the visual impression that the NW spectrum has a lower mean energy than that from the SE, we applied a version of the Mann-Whitney *U*-test. This test (Siegel 1956) is used for the comparison of

TABLE 1

FPCS OBSERVATIONS OF SILICON AND SULFUR LINES IN CASSIOPEIA A

Ion	Transition	Energy (eV)	Wavelength (Å)	Exposure ($\times 10^3$ s)	Aperture	Flux (photons cm^{-2} s^{-1})
S XV.....	$1s^2$–$1s2s$ ($^3S_1$) Forbidden	2431	5.10			
	$1s^2$–$1s2p$ ($^3P_1$) Intercombination	2450	5.06	14.8	6′ diameter	0.062 ± 0.006
	$1s^2$–$1s2p$ ($^1P_1$) Resonance	2460	5.04			
S XVI.....	$1s$–$2p$ Lyman-alpha	2621	4.73	18.4	6′ diameter	0.015 ± 0.004
Si XIII	Forbidden	1840	6.74			
	Intercombination	1856	6.68	21.7	6′ diameter	0.078 ± 0.010
	Resonance	1864	6.65			
Si XIII	...	...	...	38.6	2′ × 20′ (Position 1)	0.019 ± 0.003
Si XIII	...	...	...	42.8	2′ × 20′ (Position 2)	0.022 ± 0.003

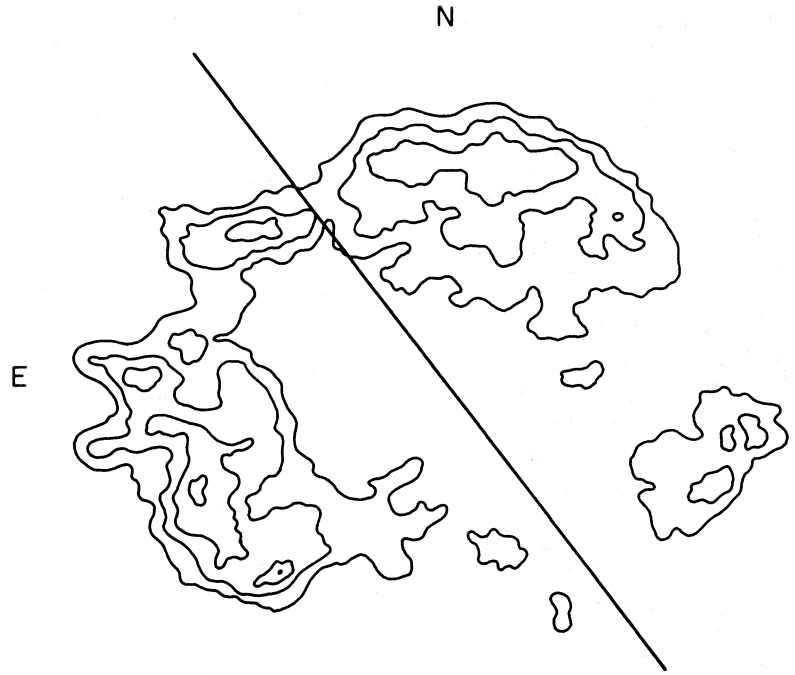

FIG. 1.—A contour intensity plot of Cas A as measured with the High Resolution Imaging device on *Einstein* (S. Murray 1982, private communication). The solid line separating the emission from the northwest from that in the southeast is approximately the division used in the analysis described in this paper.

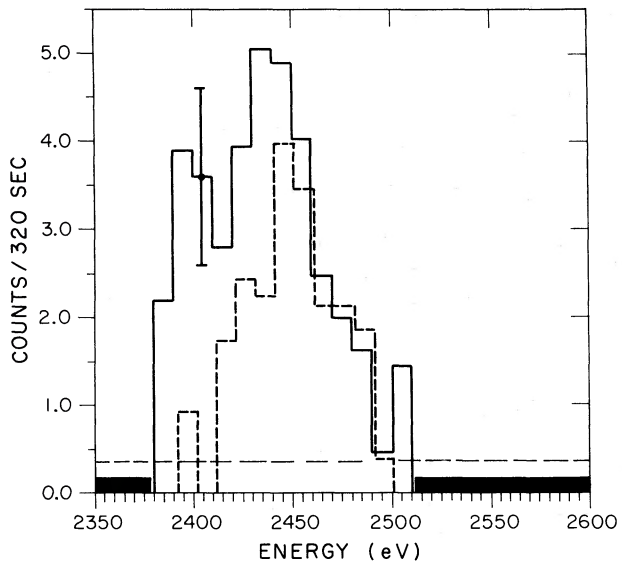

FIG. 2*a*

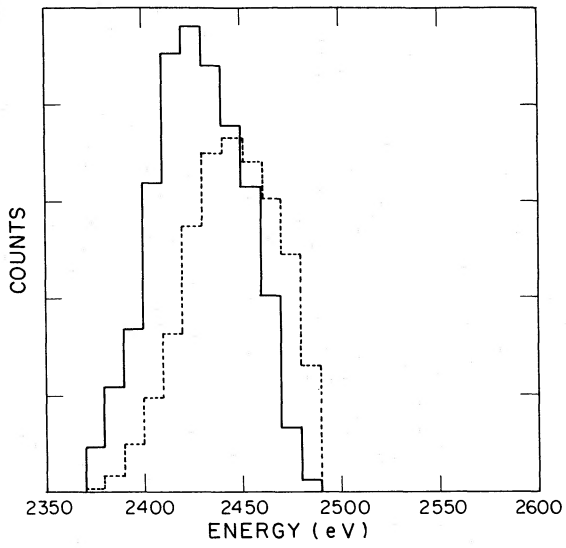

FIG. 2*b*

FIG. 2.—Spectra of the S XV helium-like lines. (*a*) Data for measurements of the SE lobe of Cas A (*dashed lines*) and for the NW lobe (*solid lines*). A typical error bar is shown. Data are shown for those energy bins in which there was significant exposure (>320 s). Heavy bars indicate the energies for which the exposure was insufficient. Instrumental background is represented by the horizontal dashed line. (*b*) A simulation of the S XV data based on the inclined ring model. Here the model parameters used were: orientation $(\phi, \gamma) = (68°, 0°)$ (this means that the ring was tilted toward the line of sight from its edge-on orientation by 68°); filling angle $\alpha = 87°$; expansion velocity $v = 5500$ km s^{-1}.

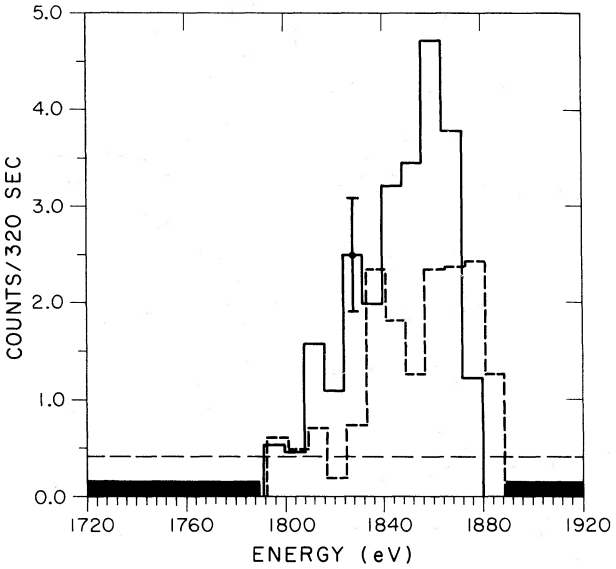

FIG. 3a

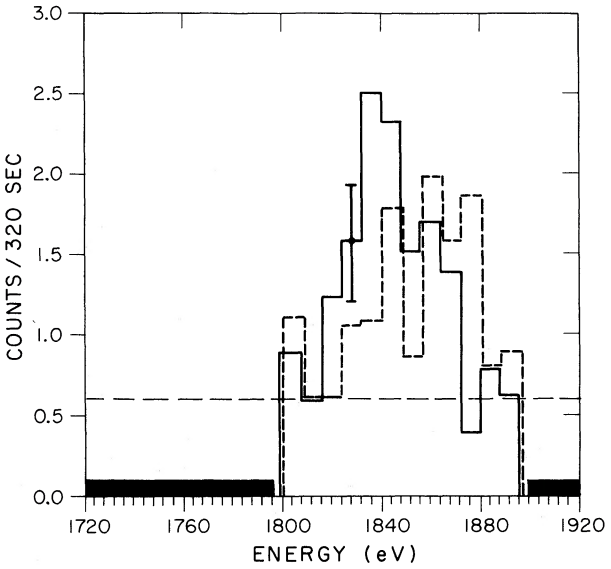

FIG. 3b

FIG. 3.—Spectra of the Si XIII helium-like lines from the SE (*dashed lines*) and NW lobes (*solid lines*) of Cas A. The background and energies with insufficient exposure are indicated as in Fig. 2*a*. Fig. 3*a* is from a single observation of Cas A for which the remnant was centered in the 6′ circular aperture of the FPCS. In Fig. 3*b*, data from two separate observations of Cas A are compared. For these observations the NW and SE lobes were examined separately by centering the lobes within the 2′ × 20′ aperture of the FPCS.

two independent statistical samples to determine if they were drawn from parent distributions with the same mean. In order to apply the Mann-Whitney test as it is usually formulated, it is necessary that each energy bin in each of the two comparison histograms have the same exposure (i.e., that the exposure histograms be identical). Rather than compare directly the NW/SE histograms (which have considerably different exposures) we compared modified histograms which were adjusted to have identical exposures. In these histograms the number of counts N_{ij} in energy bin j of histogram i (i = NW or SE) were replaced by

$$N_{ij}' = N_{ij} \times (H_{ij}/H_{\max,j}) ,$$

where H_{ij} is the exposure in bin j of histogram i and $H_{\max,j}$ is the greater of $H_{\mathrm{SE},j}$ and $H_{\mathrm{NW},i}$. This normalization is conservative, in the sense that the statistically more precise of the two N_i is degraded. Real differences between the two samples, therefore, appear to be less significant than they really are.

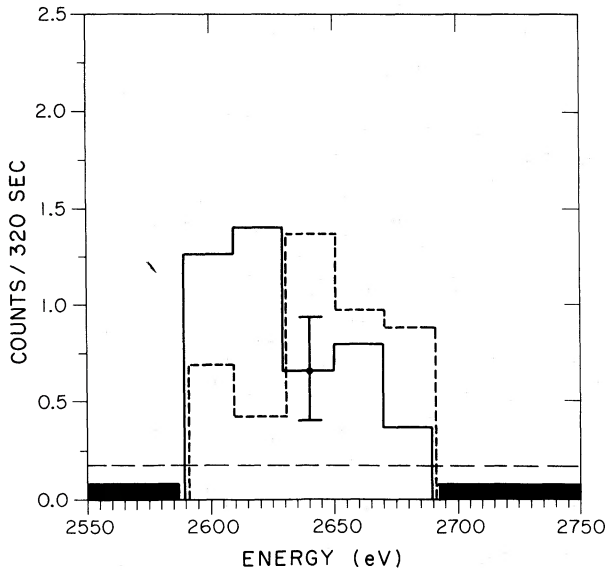

FIG. 4.—Spectra of the S XVI Lyman-alpha line of Cas A from the SE (*dashed lines*) and NW lobes (*solid lines*) of Cas A. Background and regions of insufficient exposure are indicated as in Fig. 2*a*.

The modified Mann-Whitney test was performed on the four sets of data given in Table 1. The results indicate a probability of only 10^{-5} that the observations could have arisen from parent populations in which there is no energy shift.

In order to determine the magnitude of the energy shifts, we computed the centroid of each background subtracted histogram. The energy difference between observations of the two lobes (for the same emission line) was then converted into an equivalent velocity difference [$\Delta v = (\Delta E/E) \times c$]. The results of these computations appear in Table 2 and can be compared with the instrumental resolution. The weighted mean velocity difference ($v_{\mathrm{NW}} - v_{\mathrm{SE}}$), with which all of the observations are consistent, is 1820 ± 290 km s^{-1}.

While the relative energy shift can be determined with good precision, the absolute energy shift is more difficult to compute because of fairly large uncertainties in the absolute calibration of several of the diffractors and in the rest frame values of the centroids of the helium-like lines (the relative strengths of the lines depend on plasma temperature, the state of ionization equilibrium,

TABLE 2

CENTROIDS OF SPECTRAL HISTOGRAMS

Line or Complex	Energy Range (eV)	Instrumental Resolution (σ, eV)	ΔE (SE–NW) (eV)	ΔV (km s^{-1})
S XV	2380–2510	8.2	14.8 ± 5.0	1820 ± 610
S XVI	2590–2690	13.6	23.9 ± 7.3	2720 ± 830
Si XIII (6′ aperture)	1800–1896	5.6	8.5 ± 3.6	1380 ± 580
Si XIII (2′ × 20′ aperture)	1800–1896	5.6	11.3 ± 3.0	1833 ± 470

NOTE.—Weighted mean velocity shift = 1820 ± 290 km s^{-1}.

and on questions of atomic physics which are not completely understood; e.g., see Pradhan 1982). Given the various uncertainties, the absolute velocities we compute are consistent with a picture in which the lines in the NW and SE lobes are shifted by equal and opposite amounts.

In addition to the velocity shift, we have also estimated velocity broadening for each of the lobes of Cas A by computing the root mean square deviation from the mean energy for each background subtracted histogram. This is compared to the rms deviations of simulated spectra that take account of Doppler effects, the imperfect spectral resolution of the instrument, and the blending of nearby lines (in the case of S XV and Si XIII triplets). We use the results of prelaunch calibrations to determine the instrumental energy resolutions (Table 2). These values agree with the theoretical resolution of the instrument and with the resolution observed for other lines in the spectrum of Puppis A, several of which were studied with the same crystal used for the Si XIII observations of Cas A. The relative line strengths in the helium-like triplets are set to those calculated for an equilibrium plasma of 7.2×10^6 K (Raymond and Smith 1977). We ascertained that even extreme relative line strengths such as could conceivably arise in a plasma far from ionization equilibrium (e.g., resonance = forbidden or forbidden = 0) could not change the deduced rms velocity deviation by an amount greater than the stated uncertainty.

For both the NW and SE lobes of Cas A we find an rms velocity width of ~ 2000 km s^{-1} $\pm$ 500 km s^{-1}. This corresponds to a full width at half-maximum of roughly 5000 km s^{-1}.

While we believe that the observed spectral shifts are most plausibly explained in terms of the Doppler effect, a possible alternative interpretation exists. This is that the spectra of the NW and SE lobes differ because the relative intensities of the forbidden, resonance, and intercombination lines of the helium-like triplets are different in the two lobes. The FPCS does not clearly resolve these lines, so they cannot be identified and measured separately.

This alternative explanation seems to us unlikely for four reasons. First, it does not apply to the measurements of the singlet Lyman-alpha line of S XVI (for which, however, the shift is significant at only the 2 σ level). Second, in order to have significantly different contributions from the three lines on either side of Cas A, it would be necessary for a radical difference in physical conditions to exist (e.g., rapid ionization on one side, rapid recombination on the other). Such a difference seems unlikely when the two sides are quite similar in most other respects—other line ratios (e.g., S XVI/S XV), X-ray continuum spectra, and gross morphology (Murray *et al.* 1979; Fabian *et al.* 1980). Third, the different conditions would have to have very similar nonequilibrium effects on both the Si and S triplets, yet the relevant atomic parameters for these species differ by factors of 1.5–2. Fourth, this explanation fails to account for the apparent widths of the lines, which are similar for both the NW and SE components and which are themselves indicative of high Doppler velocities.

IV. GEOMETRIC MODEL

It is clear from our data and from the images of Murray *et al.* (1979) and Fabian *et al.* (1980) that Cas A is highly asymmetric. Fabian *et al.* (1980) explored the asymmetries as projected on the sky by modeling the emission regions in numerous pie-shaped annular segments. Having no information to the contrary, they assumed that the emission per unit volume was symmetric about the plane of the sky along the line of sight. Our asymmetric Doppler velocities across the remnant give information about the structure of Cas A along this latter dimension.

Fabian *et al.* (1980) found that most of the lower temperature plasma (which is primarily responsible for the Si and S lines that we measure) is confined to a thin shell. As they note, the deficiency of X-rays from the center of the image already implies that the shell is not spherical. We use this as a starting point for a simple, geometric model that accounts roughly for the magnitude ($\Delta v \sim 1800$ km s^{-1}) and asymmetry (redshifted to the NW, blueshifted to the SE) of the velocity difference in Cas A and for the apparent widths of the lines. In addition it is consistent with the general appearance of the image produced by the HRI.

The geometric model is illustrated in Figure 5. Here the X-ray emitting gas is confined to an equatorial ring which is tilted with respect to the observer (the angles γ and ϕ define the orientation of the ring). The width of the ring is parameterized by the opening angle

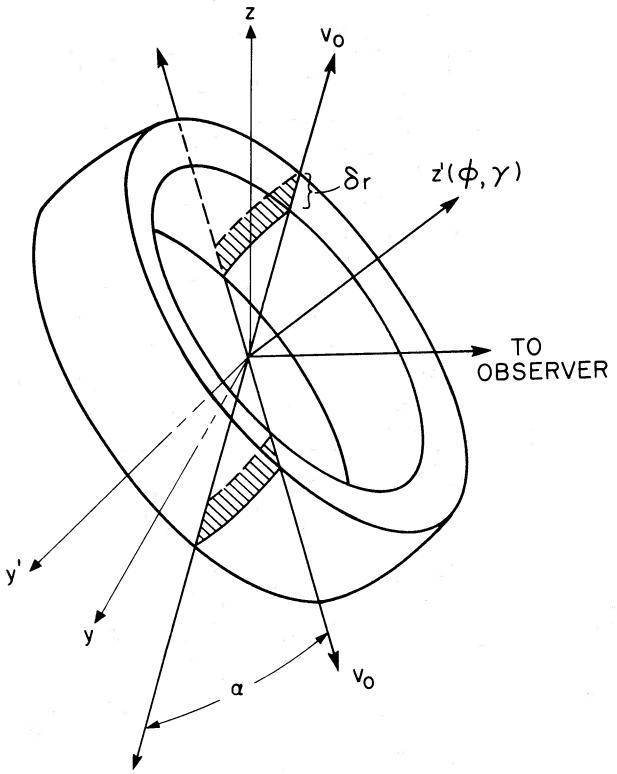

FIG. 5.—Schematic diagram of the inclined ring model of Cas A (see text). The orientation of the ring with respect to the observer is given by the angles ϕ and γ. The pole of the ring is the vector labeled z'. It is generated from the z axis (the y-z plane is the plane of the sky) by a positive rotation of magnitude ϕ about the y' axis. Similarly, the y' axis is generated from the original y axis by a positive rotation of magnitude γ about the z axis. V_0 is the velocity of expansion of the ring. We divide the ring into six azimuthal sectors and choose an X-ray intensity from each sector so as to produce an image which agrees in a general way with that seen by the HRI (Fig. 1).

α; the thickness is Δr. As α increases to 180° the model approaches a standard spherical shell. The ring is expanding radially at velocity v. To allow for azimuthal variations in intensity, we divided the HRI image into six pie-shaped wedges in the manner of Fabian *et al.* (1980). For each wedge we computed the intensity in the Si and S lines expected from that region using the densities and temperatures of Fabian *et al.* (1980) and the emissivities of Raymond and Smith (1977, 1979). We then determined the section of the inclined ring which corresponds to each wedge and assigned it the appropriate emission. In this manner we simulated the image and spectrum of Cas A for various values of the ring parameters and compared the simulations with the HRI and FPCS results. Although the simulated image does not exactly reproduce the very irregular HRI picture, it does exhibit the crude elliptical shape, shell structure, and azimuthal distribution.

As an example, Figure 2*b* shows simulated spectra for the two halves of Cas A with parameters $(\phi, \gamma, \alpha, v) = (87°, 0°, 68°, 5500 \text{ km s}^{-1})$. The input spectrum for this simulation consisted of the three lines of S XV, broadened by the resolution of the instrument. The relative intensities of the lines in the triplet were determined by assuming ionization equilibrium at a temperature $T = 7.2 \times 10^6$ K (Raymond and Smith 1977). Comparing Figures 2*a* and 2*b*, one sees reasonable agreement: the model shows an energy shift between the two halves of the remnant, the lines are broadened more than is required by the resolution of the instrument, and the emission from the SE is less intense than that from the NW. Note that the maximum line-of-sight velocity difference in this example is $2v \cos [\phi - (\alpha/2)] = 10{,}000 \text{ km s}^{-1}$, considerably greater than the velocity difference of the centroids of 1940 km s^{-1}. The centroid value is much less than the maximum value because each half of the ring contains a great deal of matter with a small projected velocity.

We find that only a certain range of parameters will produce suitable models. For example, if α, the opening angle, is too large, then the spectra from the two halves will not peak at different energies. If the angle ϕ is too small, then the projected image of the ring will be much more eccentric than is observed with the HRI. Extreme values of the expansion velocity v will produce models with incorrect Doppler shifts and/or line widths.

By comparing a grid of models with the data we can set rough limits on the range of allowed values from a qualitative comparison of the predictions of the model and the data. Figure 6 shows the region of the (ϕ, α) plane that is permitted for $\gamma = 0°$. The range of allowed expansion velocities is also displayed in Figure 6 for certain representative points in the (ϕ, α) plane. In general we find that the expansion velocity must satisfy $2000 < v < 11{,}000 \text{ km s}^{-1}$.

V. MASS AND KINETIC ENERGY OF THE X-RAY EMITTING MATERIAL

Fabian *et al.* (1980) computed masses of 15–20 $M_\odot$ for the X-ray emitting material in Cas A by deriving density and temperature maps that match the surface brightness and overall spectrum under the assumptions of pressure equilibrium throughout the remnant. As was discussed in § IV, they assumed symmetry about the plane of the sky. The true emission region is probably somewhat smaller than they assumed, but it need not be much smaller (in terms of our model the volume of the inclined ring varies as $\sin [\alpha/2]$). Since, for a given volume emission measure (density squared times volume) the mass of the X-ray emitting gas varies as the square root of the volume (or more slowly if the pressure is held fixed), the mass determined from our model can be nearly as great as that computed by Fabian *et al.* Furthermore, our measurements apply only to the low-temperature ($kT < 2$ keV) component of the gas (which contains about one-third of the mass) because the hotter regions give negligible line emission. We conclude that the deduced mass of X-ray emitting material based on the HRI image and the inclined-ring model is unlikely to fall below $\sim 10\ M_\odot$ (unless the emitting material is confined to dense clouds—see below).

This conclusion only applies to the model of Fabian

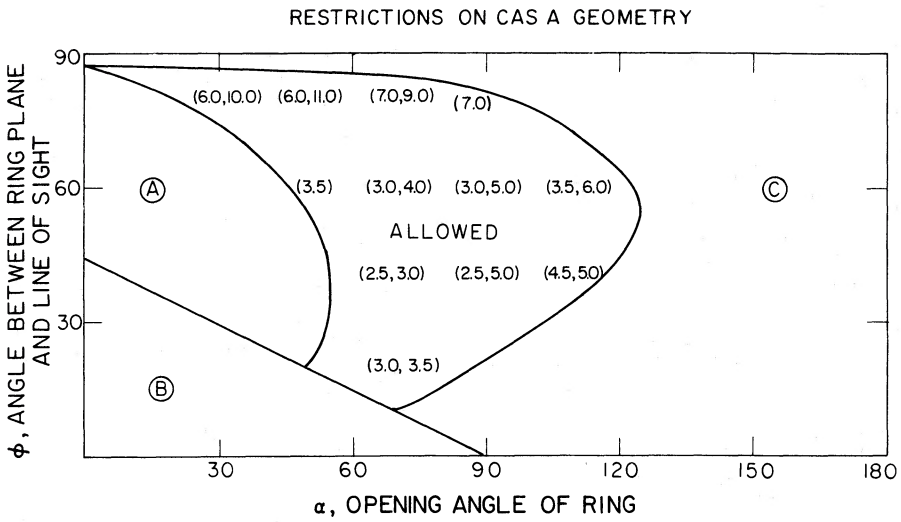

FIG. 6.—Only certain values of the parameters in the inclined ring model will produce spectra and images which are consistent with the FPCS and HRI results. Here we show qualitatively the region of the (ϕ, α) space which is consistent with the observations. The lettered regions refer to various contradictions between the model image or spectrum and the actual observations. Region A: simulated lines much narrower than observed; Region B: simulated image much flatter than HRI image; Region C: simulated lines much broader than FPCS observations. The range of permitted velocities ($\times 10^3$ km s^{-1}) is also displayed for a few representative points. For this diagram we have assumed a value of $\gamma = 0°$. The allowed regions are slightly different for $\gamma > 0°$ although the range of velocities is about the same.

et al. (1980) as modified by our observations of nonspherical symmetry. The mass of the X-ray emitting material may be considerably less if the plasma departs significantly from ionization equilibrium (Shull 1982) or if the heavy elements are considerably overabundant relative to their solar values (Long, Dopita, and Tuohy 1982).

Reasonable values for the mass and our inferred velocity of the X-ray emitting material imply that the present kinetic energy of Cas A is probably $\sim 4 \times 10^{51}$ ergs. A lower limit is $\sim 4 \times 10^{50}$ ergs. Both these values exceed the estimated internal energy of $\sim 2 \times 10^{50}$ ergs (Fabian *et al.* 1980), which indicates that the remnant cannot yet have entered its adiabatic or Sedov phase.

VI. THE NATURE OF CASSIOPEIA A

Our observations show that much of the X-ray emitting plasma in Cas A is localized, possibly in an inclined ring, and is expanding with a high velocity: $\gtrsim 2000$ km s^{-1}. This finding, together with other X-ray, optical, and radio results, strongly supports a model in which most of the X-ray emission stems from several solar masses of supernova ejecta which have decelerated little since the explosion.

Before describing a specific, self-consistent model, we review the pertinent observations and indicate how these fit into a general picture of an ejecta-dominated remnant.

a) Structure and Dynamics

The X-ray emitting plasma, which makes up most of the mass of the remnant (§ V), is relatively cool, $kT \sim 0.5$–3.5 keV for the bulk of the X-ray emitting matter (Fabian *et al.* 1980) and $kT < 2$ keV for the line-emitting plasma. Our spectroscopic observations show this material to be moving with high velocity: $v \gtrsim 2000$ km s^{-1}. Together these observations are incompatible with models in which interstellar material swept up and heated by the primary shock wave is the principal source of X-rays.[2] The temperature behind a shock of velocity v_s is $kT_s \approx 1.25\ (v_s/1000\ \text{km s}^{-1})^2$ keV (Woltjer 1972). Since the shock velocity must be greater than the bulk velocity of the X-ray emitting material behind it, our Doppler shift measurements require $kT_s > 5$ keV. There is evidence for a weak component with $kT > 15$ keV (Pravdo and Smith 1979), which may be matter behind the primary shock. However, most of the X-ray emitting material is considerably cooler than the matter heated by the primary shock.[3] The most likely interpretation for the low temperature in the high-velocity material is that heating arises from a "reverse shock" propagating inward (in a Lagrangian sense) into the outward-moving supernova ejecta (Gull, 1973, 1975; McKee 1974; Pravdo and Smith 1979). The Doppler shifts indicate the velocity of the material itself, which is higher than the propagation velocity of the reverse shock as determined from the X-ray temperature.

The X-ray image (Murray *et al.* 1979; Fabian *et al.* 1980) consists of a faint outer plateau and a much brighter inner shell. This is also most easily explained by a model in which the outer plateau is shocked inter-

[2] These observations may possibly be reconciled if the surrounding interstellar medium is extremely clumpy (see § VI*e*).

[3] We note that the presence of some plasma at $T \sim T_s$ argues against the possibility that the matter merely appears to be cool because the electron and ion temperatures are far from equilibrium (Shklovsky 1973; McKee 1974; Pravdo and Smith 1979).

stellar material and most of the X-ray emission come from reverse-shocked ejecta. The energetics of Cas A (§ V) indicate that the kinetic energy ≫ internal energy, and so favor an ejecta-dominated remnant over one which has swept up enough interstellar material to have entered its Sedov phase.

The fast-moving optical knots in Cas A represent a relatively small mass of dense material. The brightest of those knots are coincident with the bright X-ray shell and most have space velocities 4000–6000 km s^{-1} (van den Bergh 1971), comparable with that of the X-ray plasma. The space velocities of these knots cover a wide range, yet nearly all have proper motions proportional to their distances from the remnant center. The most straightforward interpretation of this result is that there has been very little deceleration of the optical material (van den Bergh and Dodd 1970). Since the velocities and positions suggest that the fast-moving optical knots are comoving with the much larger mass of diffuse X-ray emitting plasma, it is likely that none of this material has been greatly decelerated. Thus, the mass M_s of swept-up material must be small compared with the mass M_e of ejecta.

A possible eyewitness observation of the Cas A supernova event in 1680 by Flamsteed (Ashworth 1980) lends further support for an ejecta-dominated model. The date (1657) determined by linear extrapolation of the present-epoch proper motions back to the expansion center (Kamper and van den Bergh 1976) is only slightly older than the hypothetical date for the actual event. If the supernova did occur in 1680, then little deceleration has occurred and $M_e \sim 10\ M_s$ (Brecher and Wasserman 1980).

b) *Chemical Composition*

Unusually high abundances of Si, S, Ar, Ca, and perhaps other elements have been observed in the X-ray emitting plasma by Becker *et al.* (1979). The extremely strong X-ray emission lines from these elements may result in part from nonionization equilibrium conditions in the plasma (Shull 1982), but the true abundances of the silicon-group elements in Cas A nevertheless seem well above normal cosmic values. These products of nucleosynthesis are most plausibly due to a large amount of processed material ejected by the Cas A supernova.

The fast-moving optical knots also have most unusual abundances. Kirshner and Chevalier (1977) found that the composition differs dramatically from one knot to another, and that the O, S, and Ar abundances are unusually high relative to hydrogen. They have suggested that the knots are unmixed bits of ejecta from the supernova progenitor.

It is not surprising that the composition of large mass of diffuse plasma visible in X-rays should differ from that of the few shards that make up the optical knots (Fabian *et al.* 1980). The essential fact is that both are enriched in processed material, as one expects for the ejecta from a massive star.

c) *Radio Emission*

The radio map of Cas A is remarkably similar to the X-ray image (Fabian *et al.* 1980; Tuffs 1982). Proper motions of the peaks in the map imply apparent velocities of several thousand km s^{-1} in near-random directions perpendicular to the line of sight, but with a mean expansion velocity of ~ 1500 km s^{-1} (Bell 1977; Tuffs 1982). Observations at 20 cm with the VLA confirm the chaotic motion of the radio features but fail to detect a mean expansion (Angerhofer 1982).

It is most probable that the motions of the radio features do not reflect the bulk motion of the X-ray or optically emitting material. The particles which produce radio emission may be accelerated by turbulent magnetic fields, generated either through the Rayleigh–Taylor instability or through the interaction of clumpy ejecta with the surrounding medium (Chevalier 1977).

d) *Self-consistent Picture*

All of the above information on the kinematics, energetics, morphology, and composition of Cas A as determined from X-ray, optical, and radio data is consistent with a remnant composed primarily of several solar masses of supernova ejecta. This material is highly enriched in heavy elements and has been expanding at ~ 5000 km s^{-1} with little deceleration for the ~ 300 years since the supernova event. As ejecta enter the high-pressure zone behind the reverse shock, most are heated to $kT \sim 0.5$–3.5 keV, and X-ray emission results. Dense fragments of comoving material (which may be of different composition) "light up" on entering the high-pressure zone and appear for a short time as fast-moving optical knots. The radio emission may result from the acceleration of electrons by turbulent magnetic fields in the same region. Whatever the mechanism for radio production, the expansion velocity of the radio features cannot be directly linked to the velocities of the X-ray and optical emitting material.

Using a simplified reverse shock model based on McKee (1974), we can approximately match the observed age, radius, fluid velocity, and temperatures of Cas A with the following parameters: total mass of ejecta $M_e \sim 10$–$20\ M_\odot$; fraction of ejecta in reverse shocked region (i.e., the soft X-ray emitting material) $\sim \frac{1}{3}$; ambient interstellar density ~ 2–4 cm^{-3}; swept-up mass $M_x \sim 0.1\ M_e$; present velocity ~ 5000 km s^{-1}; and initial maximum velocity ~ 7000 km s^{-1}. (The latter is found by applying momentum conservation). In this picture shocked interstellar material behind the primary shock has a mass $M_s \sim 1\ M_\odot$ and a temperature $T_x > 30$ keV. It produces a negligible signal in the *Einstein* detectors and is consistent with the observations of Pravdo and Smith (1979).

The observations of X-ray Doppler shifts are most compatible with models in which the bulk of the X-ray emitting material has a nonspherically symmetric geometry, such as a ring. The asymmetries in the X-ray image and Doppler velocities could be the result of fluctuations by a factor of ~ 2 in n_0 and/or in the distribution of the ejecta (see § VII).

The wide dispersion of the radial velocities of the optical knots in the NW region fits nicely with this picture. Most of these knots show a blueshift of $\gtrsim 2000$ km s^{-1}, although several are redshifted by 4000–5000 km s^{-1} (van den Bergh 1971). The mean X-ray Doppler velocity corresponds to a redshift of $\lesssim 1000$ km s^{-1}, but in our representative model used to generate Figure 2*b* (§ IV) the closest and farthest edges of the expanding ring could have radial velocities of $v \cos(\phi \pm \alpha/2) = -2000$ km s^{-1} and $+5000$ km s^{-1}, respectively. Thus the optical knots could be identified with these edges, which, in projection, occupy nearly the same parts of the sky.

e) Alternatives

We find it difficult to reconcile the observations with a model in which $M_s \sim M_e$. In such a model one may conceivably find a velocity for the X-ray emitting matter roughly equal to that observed in the radio (although our NW/SE Doppler shifts and line widths imply larger velocities). The much higher velocities of the optical knots require an independent explanation. No model with $M_e \sim M_s$ exists that can account for the dynamics and explain the observed multiple X-ray temperatures, particularly the limit $\leq 2\ M_\odot$ on material with $kT \geq 15$ keV set by Pravdo and Smith (1979). Furthermore, the need for an additional mechanism to explain the large random motions of the radio peaks spoils the apparent economy of identifying the mean radio motions with the X-ray fluid velocity.

We find it even more difficult to construct a consistent model with $M_s \gg M_e$, i.e., the remnant is in the Sedov phase (this possibility is discussed by Fabian *et al.* 1980). We are unable to reconcile such a model with kinematics of the fast moving knots, the high velocity yet low temperatures of the X-ray emitting material, the spatial and Doppler asymmetries, the energetics of § V, indications of abundance anomalies in the X-ray spectra and the apparent youth of the remnant.

A scenario in which the interstellar medium (rather than the supernova ejecta) is the predominant source of the X-ray emission might conceivably be constructed if the medium is clumpy rather than fairly uniform. In this picture, dense ($n_c \lesssim 10^3$ cm^{-3}) clouds are shock heated to X-ray temperatures by the supernova blast wave and simultaneously accelerated to high velocities (McKee and Cowie 1975; Sgro 1975; McKee, Cowie, and Ostriker 1978). Our preliminary examination suggests that the X-ray observations could be reproduced by several solar masses of ejecta shock-heating and accelerating ~ 1000 clouds of density ~ 500 cm^{-3} and diameter ~ 0.04 pc. Whether such a model can work in detail remains to be determined.

VII. NATURE OF THE X-RAY RING

We have argued in § IV that much of the X-ray emitting matter lacks spherical symmetry and have proposed an inclined ring geometry as a simple alternative that is consistent with the X-ray image and spectrum. Presumably this geometry implies that either the supernova ejecta or the medium with which it collides must also be distributed asymmetrically.

A modest increase (by a factor of ~ 2) in the density of the interstellar medium distributed in a ring could produce a large asymmetric enhancement in the X-ray luminosity of the ejecta. If the supernova explosion were isotropic, a primary and reverse shock would occur in all directions, both on and off the higher density ring, but the reverse shock would be more fully developed and involve a larger fraction of the ejecta in the direction of the ring (the shocked fraction is proportional to $n_0^{1/2}$; McKee 1974). If the density of the ejecta were uniform (i.e., as in the models of Gull 1973, 1975), then the more well-developed reverse shock would have a higher temperature as well ($T \propto n_0$). If this temperature is associated with the ~ 1 keV material that emits the Si and S lines we observe, then even a modest density contrast would cause the remainder of the spherical volume to contain material too cool to cause significant X-ray line or continuum emission.

Analogously, if the ejecta has the more realistic radial density profile assumed by Jones, Smith, and Straka (1981), the more developed reverse shock might have already penetrated the denser material of the expanding stellar envelope whereas the less developed shock would still be propagating through the lower density material of the outer "ramp" (the exponential density gradient which connects the stellar envelope to the interstellar medium). If the density contrast of the shocked envelope with respect to the shocked ramp were greater than the density contrast in the circumsource medium, then the temperature of the shocked envelope would be lower than that of any of the shocked ramp material. The envelope could then be identified with the dense X-ray line-emitting material at $kT \sim 1$ keV, and the hotter, shocked ejecta of the ramp could explain the more symmetric X-ray "plateau", which has $kT \sim 2$–8 keV (Fabian *et al.* 1980).

We note that the proper motions of fast moving optical knots appear to show two velocity systems (Kamper and van den Bergh 1976). The knots coincident with the X-ray bright region seem to have been decelerated more than those found at larger radii, suggesting that the former have encountered more circumsource material than the latter.

A small increase in the mean density of the interstellar medium could result from mass loss from the equatorial region of the presupernova star. Such nonspherical envelopes are actually observed around late-type giant stars (Zuckerman 1980), some of which presumably evolve into supernovae.

If the observed X-ray emission arises primarily from hundreds of dense interstellar clouds, as was speculated in § V, then the observed asymmetry may be present in the distribution of the clouds.

Finally, it is possible that the supernova explosion itself may have been nonspherical. Woosley and Weaver (1981) and Bodenheimer and Woosley (1980) have argued that some massive stars may succeed in exploding only if their angular momentum allows the explosion

to be driven in the equatorial plane. This could cause an enhanced density of the ejecta in the equatorial plane which, when reverse shocked, would give rise to the X-ray ring. The Woosley model predicts that the massive progenitor stars which undergo an asymmetric explosion will eject material which is particularly rich in oxygen and the products of oxygen burning. As was discussed in § IV*b*, Cas A appears to have an overabundance of oxygen and the silicon group elements. Furthermore, other oxygen-rich SNRs also show evidence for a ring-like geometry. For example, Lasker (1980) found toroidal expansion in the optical lines of N132D (in the Large Magellanic Cloud). Also, X-ray imaging observations by Tuohy, Clark, and Burton (1982) and by Tuohy and Dopita (1982) of G292.0+1.8 and 1E0102.2−72.3 (in the Small Magellanic Cloud) revealed elliptical morphologies consistent with rings projected onto the plane of the sky.

VIII. SUMMARY

1. The X-ray spectrum of the NW portion of Cas A is redshifted with respect to that of the SE. The equivalent velocity difference between the two parts is approximately 1800 km s^{-1}, and the velocity spread within each part is $\sim$5000 km s^{-1} (FWHM).

2. A simple model consistent with the general features of the X-ray spectrum and the image of Cas A is a broad ring of matter inclined to the line-of-sight and expanding at $\sim$5500 km s^{-1}. The spectral and imaging data can be used to constrain the parameters of the ring.

3. The mass of the X-ray emitting material is probably $\lesssim 10\ M_{\odot}$ as previously determined (Fabian *et al.* 1980), and the kinetic energy is $\sim 4 \times 10^{51}$ ergs.

4. The X-ray emitting material is most probably heated by a reverse shock, as the primary shock temperatures corresponding to the observed material velocity greatly exceed the observed X-ray temperatures.

5. Although alternative scenarios cannot be excluded, the observations are most compatible with the view that Cas A is composed primarily of supernova ejecta and is still in its free-expansion stage. Within the context of this picture, plausible explanations can be found for most of the phenomena associated with Cas A.

6. The spatial and Doppler asymmetries may be caused by modest inhomogeneities in the distribution of circumsource material, which cause variations in the development of the reverse shock. Asymmetries in the ejecta themselves, as suggested for rapidly rotating, massive stars (Woosley and Weaver 1980; Bodenheimer and Woosley 1980), could equally well explain the observations.

We thank the numerous individuals at MIT's Center for Space Research and our colleagues at the Center for Astrophysics who contributed to the FPCS experiment on the *Einstein Observatory*. We particularly thank S. Murray for providing us with the HRI image of Cas A and R. Tuffs and P. Angerhofer for showing us their radio data prior to publication. We have had useful conversations with R. Becker, L. Cowie, A. Fabian, M. Johnston, T. Weaver, and S. Woosley. We thank Herman Chernoff of the MIT Statistics Center for reviewing the statistical analysis. M. E. Donahue assisted in the data analysis. We thank Brenda Parsons, Trish Dobson, Betty Sullivan, and Nancy Ferrari for their cheerful preparation of the manuscript. C. R. C. is grateful for the hospitality of the Institute of Astronomy, University of Cambridge and the support of the Royal Society through a Guest Research Fellowship.

This work was supported in part by NASA contracts NAS8-30752 and NAG-8389.

REFERENCES

Angerhofer, P. 1982, private communication.
Ashworth, W. 1980, *J. Hist. Astr.*, **11**, 1.
Baade, W., and Minkowski, R. 1954, *Ap. J.*, **119**, 206.
Becker, R. H., Holt, S. S., Smith, B. W., White, N. E., Boldt, E. A., Mushotzky, R. F., and Serlemitsos, P. J. 1979, *Ap. J.* (*Letters*), **234**, L73.
Bell, A. R. 1977, *M.N.R.A.S.*, **179**, 573.
Bodenheimer, P., and Woosley, S. 1980, *Bull. A.A.S.*, **12**, 833.
Brecher, K., and Wasserman, I. 1980, *Ap. J.* (*Letters*), **240**, L105.
Canizares, C. R., Clark, G. W., Bardas, D., and Markert, T. H. 1977, *Proc. Soc. Photo-Opt. Instrum. Eng.*, **106**, 154.
Canizares, C. R., Clark, G. W., Markert, T. H., Berg, C., Smedira, M., Bardas, D., Schnopper, H., and Kalata, K. 1979, *Ap. J.* (*Letters*), **234**, L33.
Chevalier, R. A. 1977, *Ann. Rev. Astr. Ap.*, **15**, 175.
Fabian, A. C., Willingale, R., Pye, J. P., Murray, S. S., and Fabbiano, G. 1980, *M.N.R.A.S.*, **193**, 175.
Giacconi, R., *et al.* 1979, *Ap. J.*, **230**, 540.
Gorenstein, P., and Tucker, W. H. 1976, *Ann. Rev. Astr. Ap.*, **14**, 373.
Gull, S. 1973, *M.N.R.A.S.*, **161**, 47.
———. 1975, *M.N.R.A.S.*, **171**, 263.
Jones, E. M., Smith, B. W., and Straka, W. C. 1981, *Ap. J.*, **249**, 185.
Kamper, K., and van den Bergh, S. 1976, *Ap. J. Suppl.*, **32**, 351.
Kirshner, R. P., and Chevalier, R. A. 1977, *Ap. J.*, **218**, 142.
Lasker, B. M. 1980, *Ap. J.*, **237**, 765.
Long, K. S., Dopita, M. A., and Tuohy, I. R., 1982, *Ap. J.*, **260**, 202.
McKee, C. F., 1974, *Ap. J.*, **188**, 335.
McKee, C. F., and Cowie, L. L. 1975, *Ap. J.*, **195**, 715.
McKee, C. F., Cowie, L. L., and Ostriker, J. P. 1978, *Ap. J.* (*Letters*), **219**, L23.
Murray, S. S., Fabbiano, G., Fabian, A. C., Epstein, A., and Giacconi, R. 1979, *Ap. J.* (*Letters*), **234**, L69.
Pradhan, A. K. 1982, *Ap. J.*, **263**, 477.
Pravdo, S. H., and Smith, B. W. 1979, *Ap. J.* (*Letters*), **234**, L195.
Raymond, J. C., and Smith, B. W. 1977, *Ap. J. Suppl.*, **35**, 419.
———. 1979, private communication.
Sgro, A. G. 1975, *Ap. J.*, **197**, 621.
Shklovsky, I. S. 1973, *Soviet Astr.–AJ*, **16**, 749.
Shull, J. M. 1982, *Ap. J.*, **262**, 308.
Siegel, S. 1956, *Nonparametric Statistics for the Behavioral Sciences* (New York: McGraw-Hill).
Tuffs, R. 1982, private communication.

Tuohy, I. R., Clark, D. H., and Burton, W. M. 1982, *Ap. J.* (*Letters*), **260**, L65.
Tuohy, I. R., and Dopita, M. A. 1982, *Ap. J.* (*Letters*), submitted.
van den Bergh, S. 1971, *Ap. J.*, **165**, 457.
van den Bergh, S., and Dodd, W. W. 1970, *Ap. J.*, **162**, 485.
Winkler, P. F., Canizares, C. R., Clark, G. W., Markert, T. H., and Petre, R. 1981, *Ap. J.*, **245**, 574.
Woltjer, L. 1972, *Ann. Rev. Astr. Ap.*, **10**, 129.
Woosley, S. E., and Weaver, T. A. 1981, *Ann. NY Acad. Sci.*, **375**, 357.
Zuckerman, B. 1980, *Ann. Rev. Astr. Ap.*, **18**, 263.

C. R. CANIZARES, G. W. CLARK, and T. H. MARKERT: MIT 37-515, Cambridge, MA 02139

P. F. WINKLER: Department of Physics, Middlebury College, Middlebury, VT 05723